Hexagonal Power Converter Based on Modular Multilevel Series Parallel Converter for Decoupled DC Terminals

Barrera, Felipe ; Lizana F., Ricardo; Alcaide, Abraham M.; Rivera, Sebastian

DOI
10.1109/CHILECON60335.2023.10418753

Publication date
2023

Document Version
Final published version

Published in
Proceedings of the 2023 IEEE CHILEAN Conference on Electrical, Electronics Engineering, Information and Communication Technologies (CHILECON)

2023 IEEE CHILEAN Conference on Electrical, Electronics Engineering, Information and Communication Technologies (CHILECON) | 979-8-3503-6953-3/23/$31.00 ©2023 IEEE | DOI: 10.1109/CHILECON60335.2023.10418753

Hexagonal Power Converter Based on Modular Multilevel Series Parallel Converter for Decoupled DC Terminals

Felipe Barrera
Centro de Energia
UCSC,
Concepcion 4090541, Chile
fbarrera@ing.ucsc.cl

Ricardo Lizana F.
Centro de Energia,
UCSC,
Concepcion 4090541, Chile
ricardolizana@ucsc.cl

Abraham M. Alcaide
Electronic Department,
Universidad de Sevilla,
41092 Sevilla, Spain
amarquez@ieee.org

Sebastian Rivera
Electrical Sustainable Energy - DCE&S,
Delft University of Technology,
Delft 2628 CD, Netherlands
s.rivera.i@ieee.org

***Abstract*—The Hexagonal power converter has become a suitable solution to provide high-quality voltage waveforms while achieving decoupled control of three DC terminals as well. In this case, the internal voltage balance of the different storage units is the main concern for the correct operation of the Hexagonal converter. Moreover, the Modular multilevel series-parallel converters (MMSPC) have become an interesting solution to provide higher operating voltages, reliability at a reduced cost, due to their ability to achieve a simpler internal voltage balance. In this paper, a Hexagonal power converter based on MMSPC for decoupled DC terminals is presented. The proposed system allows to implement a simple and cost-effective way to achieve a decoupled control strategy in each output of the system, to control the corresponding voltage of the system, along with maintaining the internal voltage balance of the proposed topology.**

I. Introduction

HEXAGONAL power converters are an interesting alternative for three-phase medium-voltage high-power systems. Moreover, hexagonal converters offer multiple advantages compared with other traditional power converters like the two-level voltage source converter (VSC), such as improved total harmonic distortion (THD) performance, reduced common-mode voltage, fault-tolerant capability and high-modularity and scalability [1]–[3].

The main challenge of this topology is to control the internal voltage balance of the system. If the system is internally balanced in voltage, each output of the system will operate with the correct number of voltage levels and reduced internal losses [4]–[6]. For this reason, the modular multilevel series/parallel converter (MMSPC) owns important advantages compared with the traditional power modules. The MMSPC allows not only the series interconnection among modules, but also offers their parallel interconnection. With this additional degree of freedom in the modulation stage, different control objectives can be established to achieve in an inherent way. Simpler voltage balancing between the modules without additional sensors and/or dedicated control algorithms can be achieved. This connection also leads to the reduction of the total parasitic inductance and resistance in the different energy paths [7]–[10].

In this work, a Hexagonal converter based on MMSPC for decoupled DC terminals is presented. The control strategy for achieving three decoupled DC terminals is presented, together with the implementation of the modulation strategy for the MMSPC, which allows the internal voltage balance of the system.

II. Topology description

The proposed system configuration is illustrated in Fig. 1. The proposed converter is based in six-arms, composed by (N) identical MMSPC modules. The reason behind the use of MMSPC modules is to allow internal balance among storage units without complex control or modulation techniques [9], [11], [12]. In Fig. 1, the proposed system is displayed using $N = 3$. In order to use the proposed MMSPC-based Hexagonal converter to enable three decoupled DC-stations terminals, $i.e$, the proposed system needs to control three DC voltages independently and with the ability to supply different power levels as requested by each station, as shown in Fig. 2.

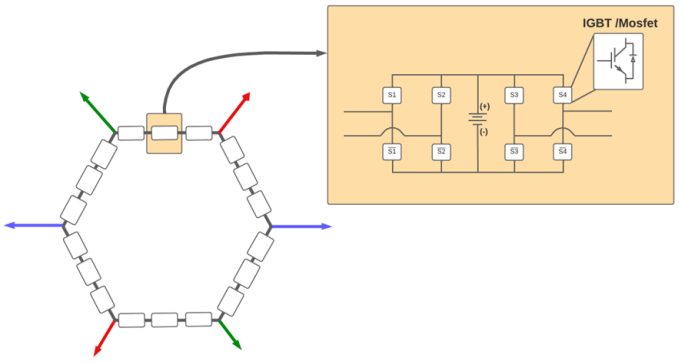

Figure 1: Hexagonal power converter based on Modular Multilevel Series parallel converter (MMSPC)

979-8-3503-6953-3/23/$31.00 2023 IEEE

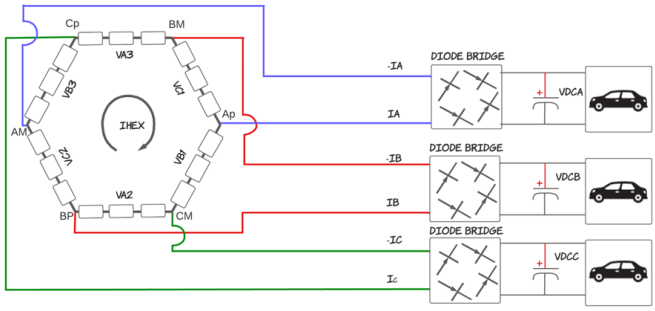

Figure 2: Hexagonal topology operating as an EV charging station.

One of the biggest challenges in the proposed system, is to maintain the internal voltage balance of the storage units incorporated in the converter. In this work, a battery is used in each MMSPC module, whose parameters are shown in Table II. Hence, the control strategy for the multi modular converter requires to maintain a balanced operation of the different batteries, which in this work will be addressed at the modulation stage, alternating the series and parallel connection of them enabled by the nature of the MMSPC modules.

III. Modelling and Control of the Hexagonal Power Converter Based on MMSPC

Each arm of the converter is modeled as a controlled voltage source plus an impedance connected in series, as shown in Fig. 3. In this model, it is assumed that the modulation imposed on the system allows the internal voltage balance of the storage units integrated in the converter, and as already mentioned, the MMSPC plays this crucial role in this topology [13].

From Fig. 3 the following equations of the converter output voltages can be obtained:

$$V_{A_pA_m} = \frac{1}{2}[V_{A2} + V_{A3} - V_{B1} - V_{B3} - V_{C1} - V_{C2} - (I_{A2} + I_{A3}) * ZL)] \quad (1)$$

$$V_{B_pB_m} = \frac{1}{2}[V_{B1} + V_{B3} - V_{C1} - V_{C2} - V_{A2} - V_{A3} - (I_{B1} + I_{B3}) * ZL)] \quad (2)$$

$$V_{C_pC_m} = \frac{1}{2}[V_{C1} + V_{C2} - V_{B1} - V_{B3} - V_{A2} - V_{A3} - (I_{C2} + I_{C1}) * ZL)] \quad (3)$$

From equations (1), (2) and (3) it is possible to generate a three-phase AC set of voltages. These voltages can be independently connected to a single-phase diode rectifier, leading to three independent DC voltages, as shown in Fig.2.

Thus, to ensure a decoupled control of each of the DC outputs of the proposed system, the control scheme described in Fig. 4 is proposed. The idea behind this control scheme

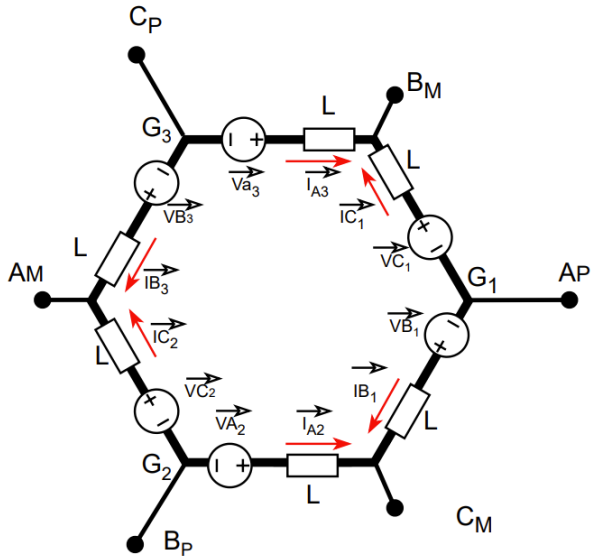

Figure 3: Hexagonal converter model

is to obtain control of the three DC voltages in a decoupled way (V_{DCA},V_{DCB} and V_{DCC}), regardless of the load that is connected to them.

In this case, the DC voltage for each output ($V_{DCx_{ref}}$) with $x = 1, 2, 3$ is defined and compared with each of the output voltages of each rectifier bridge (V_{DCA},V_{DCB} and V_{DCC}). The waveform that is generated at the output of these PI controllers is multiplied by normalized sinusoidal signals phase-shifted by 120°, in order to create the modulating signals for each arm of the proposed converter.

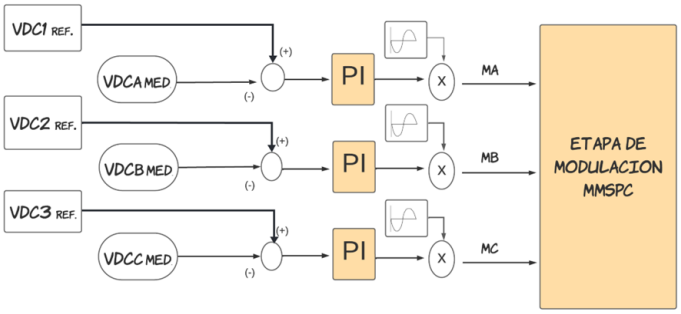

Figure 4: Hexagonal converter control scheme

The arm modulating signals are entered to the MMSPC modulation stage, as is presented in Fig. 4. This stage is based on a PS-PWM carrier modulation, where each arm modulating signal is compared with two triangular carrier waveforms, as shown in Fig. 5. If the modulation signal is greater than both carriers, the switching states of the MMSPC modules are connected in series $(+)$ mode. On the other hand, if the modulation signal is less than both carriers, the switching states of the MMSPC modules are connected in series $(-)$ mode. Finally, if the modulation signal is between

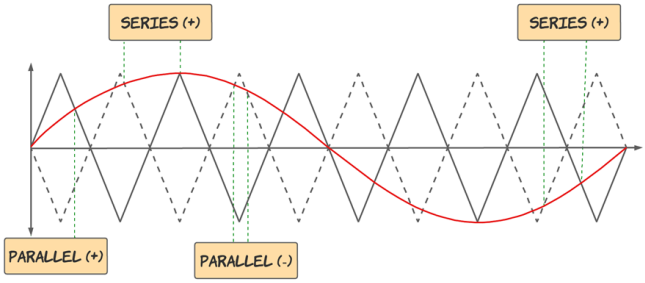

Figure 5: MMSPC modulation stage

both carriers, the switching states of the MMSPC modules are connected in parallel $(+)$ and parallel$(-)$ mode, respectively. The detail of the modulation stage of the MMSPC is presented in [13].

IV. Simulation Results

The results are obtained by modelling the hexagonal system shown in fig. 2, which has a rectification stage using a diode bridge and the control system shown in fig. 4. The simulation of the model was carried out using Mat-lab/simulink software. Different tests are performed to demonstrate the internal voltage balancing capability of the system and the feasibility of achieving decoupled DC voltage control. To demonstrate these aspects, first the analysis of the proposed Hexagonal system without load and with two capacitors and a DC voltage source is presented. In this case, the modulation stage will achieve the internal voltage balance of the modules of the same arm, to confirm the effectiveness of the MMSPC modulation stage to balance the modules. Secondly, the analysis of the proposed Hexagonal system without load with 150V lithium-ion batteries in each MMCSP module is presented to validate the correct operation of the system with batteries in each module of the system. Finally, three changes in the output DC voltage references are implemented.

Table I: Simulation Parameters

Parameter	Value
Carrier frequency of modulation framework	3 kHz
Arm Inductance L_{xy}	100 mH
Arm Resistance R_{xy}	0.1 Ω
Load Resistance R_x	500 Ω
Load Inductance L_x	10 mH
Battery type	Lithium-Ion
Nominal voltage V	150 V
Rated capacity	5.4 Ah
Initial state of charge	100 %

A. Unloaded Hexagonal system with two capacitors and one DC source in each arm of the converter

Each arm of the proposed system is composed of three MMSPC modules. In each arm, a DC source is connected to a MMSPC module and only one capacitor is connected to each of the other two in each of the branches, as can be seen in the Fig. 6 (a). In this way, it is intended to demonstrate that if the modulation of the MMSPC is well implemented, the capacitors will be charged to the equivalent value of the DC source, and the output voltages of the proposed converter ($V_{A_pA_m}$, $V_{B_pB_m}$ and $V_{C_pC_m}$) will be appreciated.

Table II: Battery parameters

Parameter	Value
Battery type	Lithium-Ion
Nominal voltage V	150 V
Rated capacity	5.4 Ah
Initial state of charge	100 %

Fig. 7 shows the voltage at the terminals of each of the phases, which are 120° phase-shifted with each other, the capacitors and internal resistors of the system are given in Table I. A total of 15 levels are shown in the generated output voltage (with a peak value of 1050 V and a voltage step between the levels of 150 V). Due to the system is operating unloaded, the current is equal to 0 A. Given the number of output voltage levels and the clear definition of each level, it can be affirmed that the modulation of the MMSPC achieves the voltage balance among the DC sources of the modules, which in this case were a battery and two capacitors.

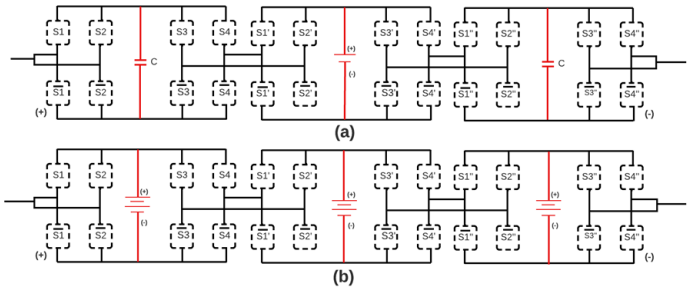

Figure 6: The arm of the hexagonal system (a) MMSPC with DC source and capacitor (b) MMSPC with batteries

B. Hexagonal system with battery in each MMSPC modules and no load

In Fig. 8 shows the representation of each of the phases considering that each of the branches of the hexagonal system is composed of three MMSPC converters and each of these has a battery as can be seen in Fig. 6 (b) . In total, the hexagonal system has 18 batteries. The battery curves are composed of three important regions; the first one is the exponential area where the maximum charge value of the battery is found (Fully charged), it is important to highlight that the time that a battery can be maintained in this state depends on the intrinsic characteristics of each battery, the second area is the nominal voltage area of the battery and the third area is the discharge stage.

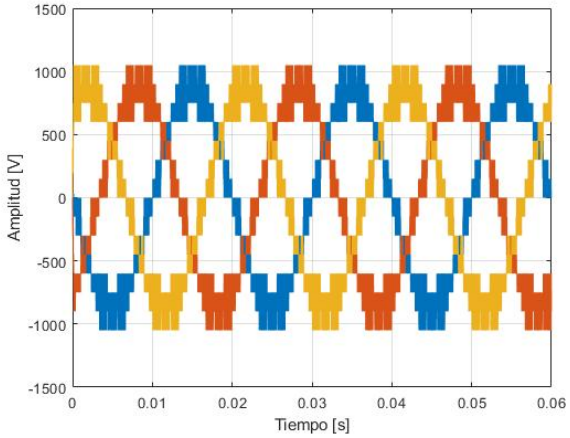

Figure 7: No load voltage with DC source

For this reason, in Fig. 8 having a nominal voltage per battery of 150 V, a higher voltage amplitude is obtained with a peak of -1226.74V and 1226.74V with a total of 15 levels. The peak value of the batteries is approximately 14.38% higher than the nominal voltage, leading to an increased voltage step of 175.24 V.

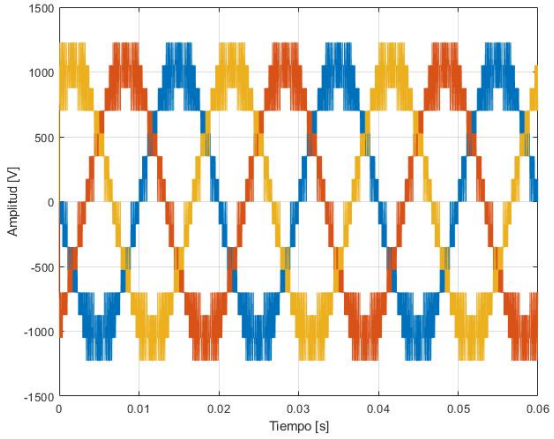

Figure 8: No load voltage with batteries

C. Hexagonal system with changes in the output DC voltage references

To study the different responses of the proposed Hexagonal system, three changes in the output DC voltage references were generated. Keeping the resistive load values presented in table I

In Fig. 9, it is possible to appreciate the three DC voltages of the system's outputs, $i.e.$ after a rectification stage based on diode bridges in each of the phases. At the beginning, the system starts with voltage reference equal to 700 V. At $t = 3$ s, the DC voltage reference changes to 500 V and finally, at $t = 6$ s, the DC voltage reference changes to 300 V. From Fig. 9, it is possible to appreciate that the three output voltage signals follow the references, and therefore, demonstrate the correct control of each DC output voltage port.

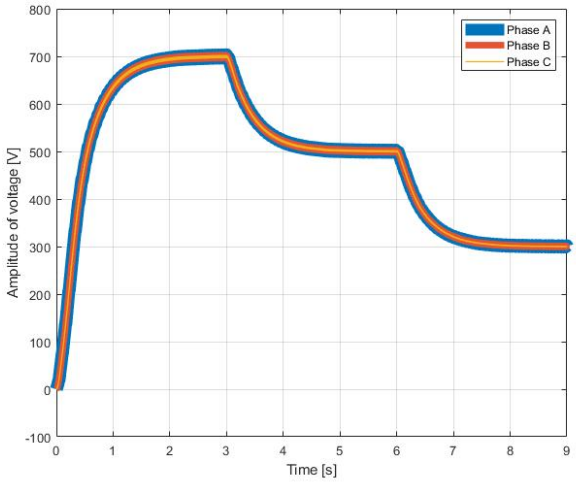

Figure 9: DC voltage of the load

In Fig. 10, it is possible to appreciate the value of the current that can be obtained in the load after the rectifying process. From this figure, when a DC voltage reference occurs, the value of the current decreases. At the beginning, when the voltage is 700 V the current is 1.4 A, but when the voltage drops to 500 V the current drops by 28.57% reaching the value of 1 A, continuing with this when the voltage drops again to 300 V the current drops to 0.6 A. This behavior is the same in each phase of the system since the loads of the three phases are the same. Finally, Fig. 11 a zoomed graph of the DC current waveforms to highlight their waveforms and details.

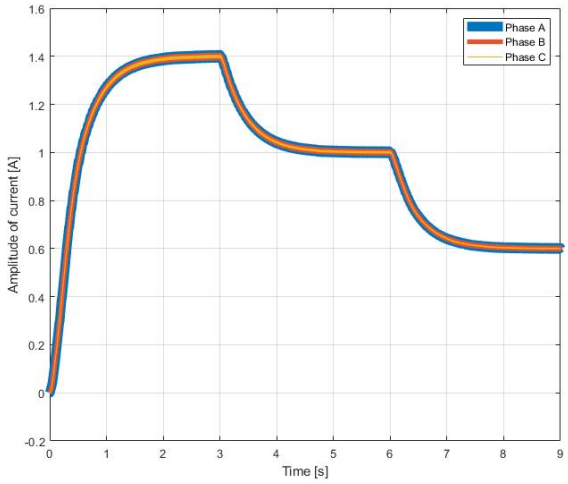

Figure 10: DC current of the load

Then, Fig. 12 and Fig. 13 show the output AC voltages and currents of the proposed converter, respectively. From these figures, it can be observed that the amplitude dynamics

imposed by the changes of DC voltage references of each of the output DC ports predominates.

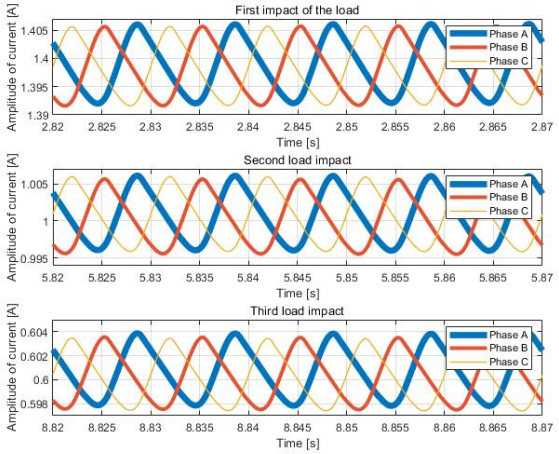

Figure 11: Zoom of DC currents waveform.

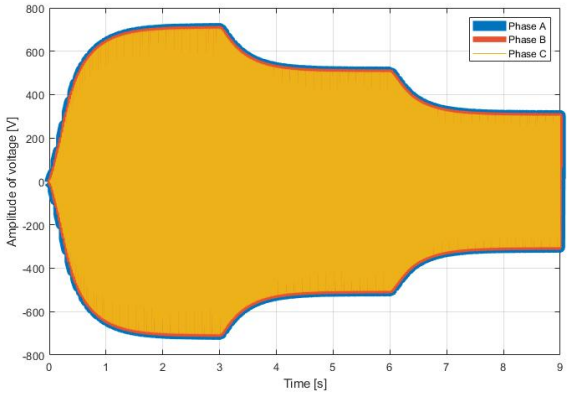

Figure 12: AC voltage hexagonal converter

Moreover, in Fig. 14, a zoomed view of the current waveforms is provided. These currents for each phase of the system have typical characteristics of voltage rectifier diode bridges that have a capacitor such as DC-link, so they have a significant harmonic content. For this reason, the use of this type of solution allows mitigating the effect of this type of system, since this current is generated by the storage elements of the converter and not directly by the electrical grid.

Like a second validation stage, the decoupled control of each DC port is validated. From Fig. 15, a change in the DC-voltage reference is implemented. The DC-voltage references changes from 400V to $V_{DCA_{ref}} = 375V$, $V_{DCB_{ref}} = 400V$ and $V_{DCC_{ref}} = 350V$. The proposed system allows a decoupled control of the DC-terminal, like is shown in Fig. 15.

D. Analysis of the behavior of batteries with changes in the output DC voltage reference

Using the voltage values presented in the previous section. In Fig. 16 shows the state of charge (SOC) of the batteries

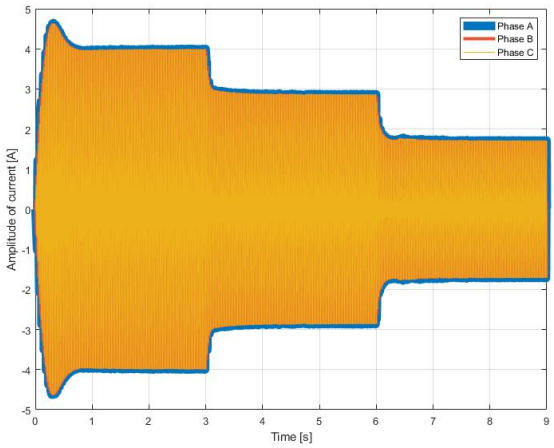

Figure 13: AC current hexagonal converter

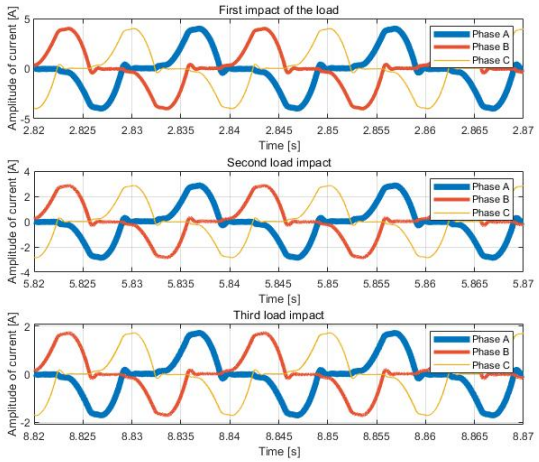

Figure 14: Zoom of AC currents waveform.

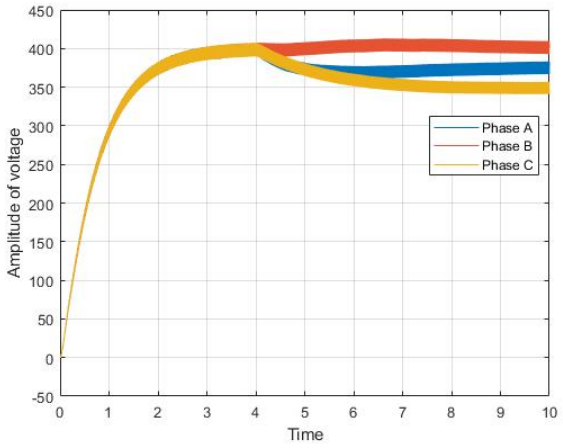

Figure 15: Voltage with load change

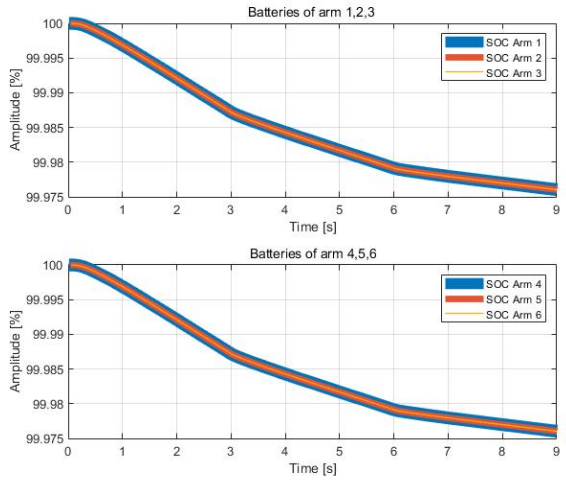

Figure 16: State of charge %

present in the arms of the system. The upper part shows the SOC of arms 1, 2 and 3, and the lower part shows the SOC of the arms 4, 5 and 6. From this point on, the discharge of the batteries is linear. From Fig. 16, it is possible to obtain that in the interval between $t = 0$ s to the first impact in the DC voltage reference, that is generated at $t = 3$ s, the SOC in all the batteries are are equitably reducing with a defined rate. For the second change in the DC voltage reference, the rate of change in the SOC is lower, this because the load needs less energy from the batteries. The same occurs in the last interval of the Fig. 16. It is important to highlight that both, the lower arms of the system and the upper ones, present the same discharge behavior, due to the internal voltage balance strategy.

V. Conclusions

This paper proposed a Hexagonal power converter based on MMSPC for decoupled DC terminals. The use of MMSPC modules in the system allows the internal voltage balance of the different storage units that are connected in each module of the proposed system. This internal balance is implemented in the modulation stage and does not need any additional sensors or control loop.

The proposed control strategy allows to control the DC voltage of each DC terminals of the system. Due to the internal voltage balance by the MMSPC modules achieve the internal voltage, it is possible to achieve the correct operation of each arm of the Hexagonal power system.

Simulation results validate the control strategy and the internal voltage balance, in order to use these results as a milestone for the implementation of the proposed system in different applications like EV charging stations or Back-up power systems.

VI. Acknowledgment

This work was supported by the following projects from the Agencia Nacional de Investigación y Desarrollo (ANID): FONDECYT-R Grant No. 1230306, REDES-PCI 190108, AC3E (ANID/Basal/FB0008), Fondo de Actividades Académicas FAA-UCSC, Centro de Energía UCSC and SERC Chile (ANID/FONDAP/1522A0006). Abraham M. Alcaide gratefully acknowledges to the Contratación de Personal Investigador Doctor. (Convocatoria 2019) 43 Contratos Capital Humano Línea 2. Paidi 2020, supported by the European Social Fund and Junta de Andalucía. and the Spanish Ministry of Universities under the grant Jose Castillejo 2023, CAS22/00425.

References

[1] J. Rodriguez, S. Bernet, B. Wu, J. O. Pontt, and S. Kouro, "Multilevel Voltage-Source-Converter Topologies for Industrial Medium-Voltage Drives," *IEEE Trans. Ind. Electron.*, vol. 54, no. 6, pp. 2930–2945, Dec 2007.

[2] S. Kouro, M. Malinowski, K. Gopakumar, J. Pou, L. G. Franquelo, B. Wu, J. Rodriguez, M. A. Perez, and J. I. Leon, "Recent Advances and Industrial Applications of Multilevel Converters," *IEEE Trans. Ind. Electron.*, vol. 57, no. 8, pp. 2553–2580, Aug 2010.

[3] L. G. Franquelo, J. Rodriguez, J. I. Leon, S. Kouro, R. Portillo, and M. A. M. Prats, "The Age of Multilevel Converters Arrives," *IEEE Ind. Electron. Mag.*, vol. 2, no. 2, pp. 28–39, June 2008.

[4] F. Rong, S. Xu, L. Pan, and Z. Sun, "Transformerless grid connected control of wind turbine based on h-mmc," *IEEE Journal of Emerging and Selected Topics in Power Electronics*, vol. 10, no. 2, pp. 2126–2137, 2022.

[5] P. Wang, F. Liu, J. Gong, W. Liu, F. Zhu, and Z. Chen, "Regenerated energy recycling between two motors of asynchronous mode driven by hexagonal cascaded multilevel converter," in *2017 IEEE Applied Power Electronics Conference and Exposition (APEC)*, 2017, pp. 558–562.

[6] M. Roknuzzaman and S.-I. Hamasaki, "Control of loop power controller applying hexagonal modular multi-level converter," in *2022 International Symposium on Power Electronics, Electrical Drives, Automation and Motion (SPEEDAM)*, 2022, pp. 730–735.

[7] F. Helling, S. Götz, A. Singer, and T. Weyh, "Fast modular multilevel series/parallel converter for direct-drive gas turbines," in *2015 IEEE NW Russia Young Researchers in Electrical and Electronic Engineering Conference (EIConRusNW)*, Feb 2015, pp. 198–202.

[8] C. Wang, Z. Li, D. L. K. Murphy, Z. Li, A. V. Peterchev, and S. M. Goetz, "Photovoltaic Multilevel Inverter with Distributed Maximum Power Point Tracking and Dynamic Circuit Reconfiguration," in *2017 IEEE 3rd International Future Energy Electronics Conference and ECCE Asia (IFEEC 2017 - ECCE Asia)*, June 2017, pp. 1520–1525.

[9] S. M. Goetz, Z. Li, X. Liang, C. Zhang, S. M. Lukic, and A. V. Peterchev, "Control of Modular Multilevel Converter With Parallel Connectivity - Application to Battery Systems," *IEEE Trans. Power Electron.*, vol. 32, no. 11, pp. 8381–8392, Nov 2017.

[10] R. L. F., S. Rivera, Z. Li, J. Luo, A. V. Peterchev, and S. M. Goetz, "Modular multilevel series/parallel converter with switched-inductor energy transfer between modules," *IEEE Transactions on Power Electronics*, vol. 34, no. 5, pp. 4844–4852, 2019.

[11] S. M. Goetz, A. V. Peterchev, and T. Weyh, "Modular Multilevel Converter With Series and Parallel Module Connectivity: Topology and Control," *IEEE Trans. Power Electron.*, vol. 30, no. 1, pp. 203–215, Jan 2015.

[12] H. Bahamonde I., S. Rivera, Z. Li, S. Goetz, A. Peterchev, and R. Lizana F., "Different parallel connections generated by the modular multilevel series/parallel converter: an overview," in *IECON 2019 - 45th Annual Conference of the IEEE Industrial Electronics Society*, vol. 1, 2019, pp. 6114–6119.

[13] Z. Li, R. Lizana, S. Sha, Z. Yu, A. V. Peterchev, and S. Goetz, "Module implementation and modulation strategy for sensorless balancing in modular multilevel converters," *IEEE Transactions on Power Electronics*, pp. 1–1, 2018.